Optical Engineering

SPIEDigitalLibrary.org/oe

Analytical model for the electro-thermal feedback effect in a microbolometer infrared focal plane array

Seung-man Park
Seungoh Han
Hee Chul Lee

SPIE

Analytical model for the electro-thermal feedback effect in a microbolometer infrared focal plane array

Seung-man Park,[a,*] Seungoh Han,[b] and Hee Chul Lee[c]
[a]Hoseo University, Department of Defense Science and Technology, 79-20 Hoseoro Babang-eup, Asan, Choongnam 336-795, Republic of Korea
[b]Hoseo University, Department of Robotics Engineering, 79-20 Hoseoro Babang-eup, Asan, Choongnam 336-795, Republic of Korea
[c]Korea Advanced Institute of Science and Technology, Department of Electrical Engineering, 335 Gwahangno, Yuseong-gu, Daejeon 305-701, Republic of Korea

Abstract. An analytical model for the electro-thermal feedback effect in a microbolometer infrared focal plane array is presented. The presented model is the integrated optical-electro-thermal model, in which the electro-thermal feedback effect incorporated with the response of incident IR can be described. In addition, since the model is based on physics, the model parameters also have their own physical meaning. This analytical model can be easily utilized to describe the temperature increase caused by the applied heat sources and has a unique feature describing capability of optical-electro-thermal analysis in a quasi-steady-state, which can hardly be performed with thermal analysis tools based on the finite element method. The model shows that the temperature of the microbolometer in this study can be increased 7.1% to 18.6% more by the electro-thermal feedback effect. [DOI: 10.1117/1.OE.53.4.043104]

Keywords: electro-thermal feedback; microbolometer; infrared focal plane array; analytical model; integrated model.

Paper 131375 received Sep. 6, 2013; revised manuscript received Feb. 4, 2014; accepted for publication Mar. 6, 2014; published online Apr. 3, 2014.

1 Introduction

Uncooled microbolometer infrared focal plane array (IRFPA) technology has extended its application to the small-size, low-weight, low-power, and low-cost IR systems.[1–3] As the density of IRFPA has rapidly increased, several technical challenges, such as process technology, optical fill-factor, thermal isolation, and the thermal drift of their characteristics, have emerged.[4–11] The accurate performance prediction of the high-density microbolometer IRFPA is also one of the emerging challenges.[8–16] In order to make a reasonable performance prediction of a highly optimized and high-density microbolometer IRFPA, the correct understanding of the electro-thermal phenomena that occur in a microbolometer IRFPA is essentially required. Since the electro-thermal effect is related to the temperature change and the electronic state change of a sensing material, this effect is inherent in a thermal detector like the microbolometer. Hence, the correct understanding of the electro-thermal effect leads not only to a more accurate signal prediction in the development, but also to the proper use of an IRFPA in the application period.[13–18]

In this article, two analytical models for the electro-thermal feedback effect in the microbolometer IRFPA are presented. The electro-thermal feedback effect starts when the bias is applied to read the resistance change of the microbolometer in IRFPA. Once the bias is applied, the bias heat, which is inversely proportional to the resistance of the microbolometer for a constant voltage bias, is produced in a sensing material. This bias heat leads to a rapid temperature increase in the microbolometer. Since the negative temperature coefficient of resistance (NTCR) of IR sensing materials such as VOx and a-Si is used for most microbolometer technology, the bias heat makes the resistance decrease further. Once again, the further the resistance of the microbolometer decreases, the more the bias heat is produced. Therefore, this electro-thermal process is a positive feedback. The electro-thermal feedback increases the apparent signal of the microbolometer IRFPA. Thus, the measured signal voltage may be larger than that predicted without considering the electro-thermal feedback. In order to reduce this positive feedback effect, the biasing time should be decreased. However, decreasing the bias time, which determines the integration time, is not desirable since it increases the noise bandwidth, and hence the noise equivalent temperature differenc.[15–17] As a result, it is of high importance to understand the electro-thermal feedback effect as correctly as possible.

*Address all correspondence to: Seung-man Park, E-mail: smanpark@hoseo.edu

2 Electro-Thermal Feedback Models

Since we are interested in the electro-thermal feedback, our primary goal is to find a proper solution to the heat balance equation of a microbolometer in the case, where a constant IR radiation and a voltage bias are applied simultaneously to a microbolometer. The heat balance equation of a microbolometer is given by

$$H\frac{d\Delta T}{dt} + K \cdot \Delta T = P, \tag{1}$$

where H and K are the heat capacity and the thermal conductance, respectively.[13–19] $\Delta T = T_d - T_a$. Also, T_d, T_a, and P are the detector temperature, the constant ambient temperature, and the heat source, respectively.

If P is constant in time, the solution to Eq. (1) is given by the following equation:

$$\Delta T = \frac{P}{K}(1 - e^{-t/\tau_{\text{th}}}) \cong \frac{P}{H}t, \tag{2}$$

where $\tau_{\text{th}} = H/K$ is the thermal time constant. The last expression is valid only for $t \ll \tau_{\text{th}}$. The electro-thermal feedback effect is not included in Eq. (2) and this equation has been used to describe the temperature change with applied bias with a slight modification of the bias heat term to be constant as the initial power. We call Eq. (2) the conventional linear (CL) model.

As the bias is applied, the P in Eq. (2) is not constant since the bias heat is time dependent. During the constant voltage bias, usually with a pulse form, P can be expressed as follows, in which the bias heat is decomposed into time dependent and independent terms.

$$P = \varepsilon\phi_e + \frac{V_{\text{Bias}}^2}{R_d} \cong \left(\varepsilon\phi_e + \frac{V_{\text{Bias}}^2}{R_{d0}}\right) - \frac{\alpha V_{\text{Bias}}^2}{R_{d0}}\Delta T, \tag{3}$$

where α, ε, and ϕ_e are the temperature coefficient of resistance of a sensing material, the IR absorption coefficient, and the incident IR power, respectively. The relationship of $R_d = R_{d0}(1 + \alpha\Delta T)$ is also used. Also, the last approximation in Eq. (3) is valid for $\alpha\Delta T \ll 1$. By putting Eq. (3) into Eq. (2), we can get the following equation:

$$\Delta T = \left(\varepsilon\phi_e + \frac{V_{\text{Bias}}^2}{R_{d0}}\right)\frac{t}{H}\left(1 + \alpha\frac{V_{\text{Bias}}^2}{HR_{d0}}t\right)^{-1}. \tag{4}$$

From Eq. (4), one can see the feedback characteristic of bias heat. If the incident IR radiation can be negligible, then Eq. (4) becomes the exact same form of a feedback amplifier gain expression[20] with a loop gain of $\alpha[(V_{\text{Bias}}^2)/(HR_{do})]t$. The only difference is that the loop gain is negative because of the NTCR of the sensing material, so the electro-thermal feedback modeled by Eq. (4) is a positive feedback, as previously mentioned, and is as intuitive as that in the circuit theory. We call Eq. (4), the feedback amplifier gain (FAG) model, for our discussion.

Another approach is possible. With rearrangement after putting Eq. (3) into Eq. (1), one can get an easily solvable equation as follows:

$$H\frac{d\Delta T}{dt} + K_{\text{eff}} \cdot \Delta T = P_0, \tag{5}$$

$$K_{\text{eff}} = K + \frac{\alpha V_{\text{Bias}}^2}{R_{d0}}, \tag{6}$$

$$P_0 = \varepsilon\phi_e + \frac{V_{\text{Bias}}^2}{R_{d0}}, \tag{7}$$

where, K_{eff} and P_0 are the effective thermal conductance (ETC) and the time independent heat source, respectively. Whereas the only time independent source term in Eq. (5) with constant incident IR radiation power is treated as a heat source, the time-dependent source term is treated as the term contributing to the ETC. As expected, the solution to Eq. (5) can be found as follows:

$$\Delta T = \frac{P_0}{K_{\text{eff}}}(1 - e^{-t/\tau_{\text{eff}}}), \tag{8}$$

where τ_{eff} is the effective time constant defined by $\tau_{\text{eff}} = H/K_{\text{eff}}$. Although Eq. (8) has the exact same form as Eq. (2), the increasing shapes in temperature are quite different. This difference stems from the fact that K_{eff} is less than K, even can be a negative value, then so do τ_{eff}. The physical meaning of the K_{eff} can be interpreted as follows. If $K_{\text{eff}} < 0$, then the heat flows into the microbolometer from the ambient. Accordingly, the heat piled up on the microbolometer will rapidly increase, so this piling up of heat will lead to the rapid increase of its temperature. So, ΔT exponentially increased as expected in Eq. (8). If $K_{\text{eff}} = 0$, then the heat flowed out to the ambient is precisely balanced with the heat produced by time dependent bias. Accordingly, the heat piled up on the microbolometer will be increased by an amount of time independent heat source P_0, so ΔT is linearly dependent on time with a constant heat source P_0, as in Eq. (5). We will call Eq. (8), the ETC model.

Two models were derived from the heat balance equation of a microbolometer. Here, one question arises: Which one is better? In the derivation of Eq. (4), three assumptions were made. The first was $t \ll \tau_{\text{th}}$, the second was $\alpha\Delta T \ll 1$, and the third P was constant in Eq. (2). The first two are very likely. The third is also plausible, in that the mitigation of this assumption was made by quietly inserting the time dependent term of Eq. (3) into Eq. (2). On the other hand, in the derivation of Eq. (8), only the second one was made. So, it can be said that the ETC model is more physical with less assumptions in it. Although Eq. (4) is more intuitive, Eq. (8) is more physical.

3 Applications of the Models and Discussion

In order to demonstrate the utilization of two analytical models for describing the electro-thermal feedback effect, the FAG model of Eq. (4), the ETC model of Eq. (8), and the CL model of Eq. (2) were applied to a typical microbolometer IRFPA. The characteristics of the microbolometer IRFPA used for this study are summarized in Table 1.[16–19]

The temperatures of the microbolometer calculated by the CL, FAG, and ETC models, respectively, are shown in Fig. 1. It is presumed that the microbolometer is illuminated by an incident IR radiation from a 35°C extended black body source. The inset of Fig. 1 shows the temperature changes of the microbolometer over the first six frame times. Over one frame time of T_f, only for the first 100 μs, the bias is applied to the microbolometer, so the temperature rapidly increases for this biasing time. After the biasing time, the microbolometer is cooled down naturally as the bias heat is dissipated to the substrate mainly by conduction. After three to five frame times, the maximum temperature is reached at the end of the biasing time, while the saturated cooling temperature also reached at the end of cooling time. We call this state the quasi-steady-state of a microbolometer. Figure 1 shows the solution to the heat balance equation of the microbolometer with an electro-thermal feedback effect over several frames up to the quasi-steady-state condition. This capability to describe the quasi-steady-state condition is the most unique feature of our model, distinguishing itself from other thermal analysis tools. The temperatures at the end of the biasing time in the quasi-steady-state calculated with the

Table 1 The characteristic parameters of a microbolometer infrared focal plane array (IRFPA) used for this study.

Parameter	Symbol	Value	Unit	Other
		A bolometer in FPA		
Pixel pitch		25×25	μm^2	
Optical fillfactor		0.7		
Thermal conductance	K	3×10^{-8}	W/K	
Heat capacity	H	3×10^{-10}	J/K	
IR absorption coefficient	ε	0.8		
Resistance	R_{d0}	170	kΩ	At 298 K
Temperature coefficient of resistance (TCR)	α	−0.02	1/K	
		Reference bolometer		
Thermal conductance	K	1×10^{-3}	W/K	
Heat capacity	H	1.2×10^{-9}	J/K	
IR absorption coefficient	ε	0		Optical blind
Resistance	R_{d0}	155	kΩ	At 298 K
TCR	α	−0.02	1/K	
# Ref. bolometers per col.		1	ea	
		IRFPA		
Format		320×240		
Bias voltage	V_{Bias}	2	V	const. vol. pulse
Readout type	C_{int} T_{int}	30 100	pF μs	columnwise readout with CTIA
Frame time	T_f	33	ms	
Incident IR power	Φ_e	24.3	nW	
Ambient temperature	T_a	298	K	constant

FAG and ETC models are larger than that with CL, in which the electro-thermal feedback effect was not considered. Whereas the temperature change is 8.90 K calculated with CL, those are 10.55 and 9.53 K with the FAG and ETC models, respectively. Thus, it can be seen that the temperatures from the FAG and ETC models are 18.6% and 7.1% higher than that from CL. These results of the electro-thermal feedback effect may be too large to overlook for making more precise tradeoffs among their performance parameters of a high-density microbolometer IRFPA in both the development and application periods.

The modeled resistances of the microbolometer are shown in Fig. 2. The inset of Fig. 2 shows the resistance changes of the microbolometer over the first six frame times like in Fig. 1. In the quasi-steady-state, the resistance changes calculated with the FAG and ETC models are larger than that with CL. While the resistance change is 30.4 kΩ calculated

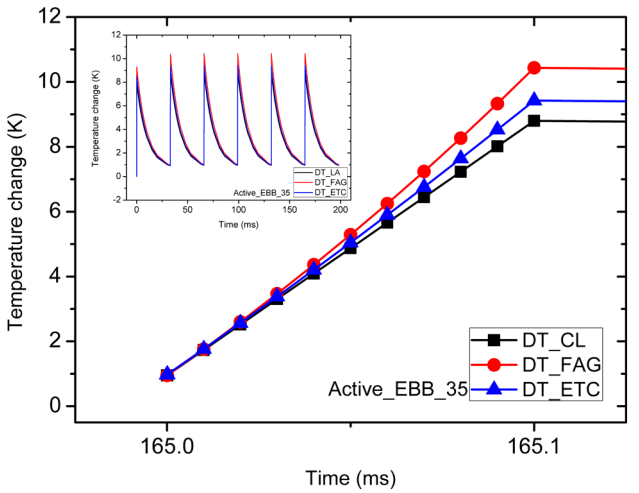

Fig. 1 Temperature changes calculated with feedback amplifier gain (FAG), effective thermal conductance (ETC), and conventional linear (CL) models, respectively.

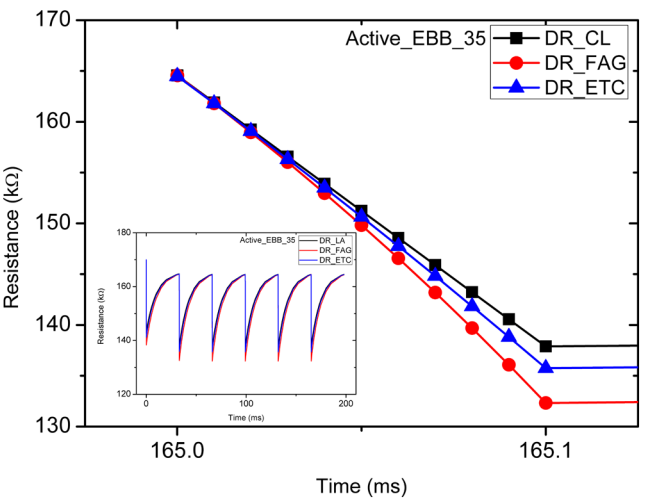

Fig. 2 Resistance changes calculated with FAG, ETC, and CL models, respectively.

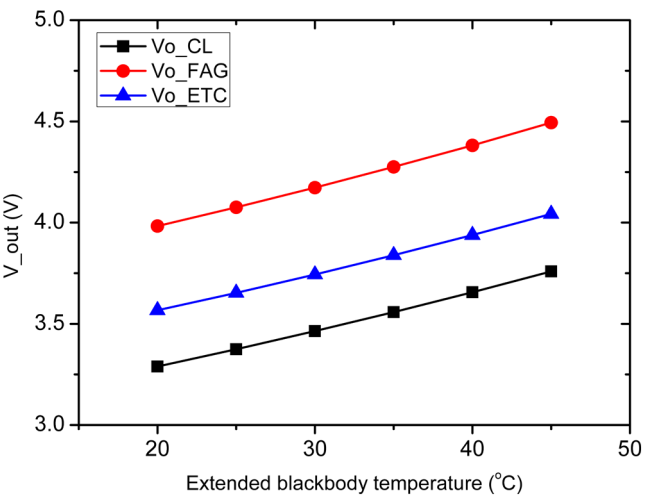

Fig. 3 Infrared response signals calculated with FAG, ETC, and CL models, respectively.

with CL, those are 42.4 and 35.5 kΩ with the FAG and ETC models, respectively. Thus, it can be seen that the resistance changes by considering the electro-thermal feedback effect are 17.3% and 6.7% larger than that from CL. The clear results of the electro-thermal feedback models are shown in Fig. 1 for the temperature and in Fig. 2 for the resistance of the microbolometer.

The IR response signals for each temperature of an extended blackbody source can be predicted with the model.[16–19] The IR response signals can be predicted from the resistance changes calculated with each model. Figure 3 shows the predicted IR response signals of the previous microbolometer IRFPA of Table 1. Here, it is assumed that the microbolometer IRFPA has a columnwise readout with a capacitive transimpedance amplifier as a column amplifier, as indicated in Table 1.[19,21] The IR response signals from the FAG and ETC models, in which the incident IR radiation incorporated with the electro-thermal feedback effect are considered, are larger than that from CL, in which only the IR radiation is considered. This means that the IR response signals are affected by the electro-thermal feedback effect. Since most IR imaging systems utilizing modern IRFPA technologies to get a high quality image are operated after proper nonuniformity corrections (NUC), the relative response signals are more important. The relative temperature responses extracted from the signals of 20°C and 35°C are 19.5, 18.1 mV/K with the FAG, ETC models, respectively, while 17.9 mV/K with CL. Compared with the result without an electro-thermal feedback effect, the relative responses with the FAG and ETC models are nearly the same as that with CL. This means that most of the electro-thermal feedback effect can be eliminated by NUC. However, the remaining parts still can affect the nonuniformity of an image even after NUC.

4 Conclusion

The presented analytical model is the integrated optical-electro-thermal model, with which the electro-thermal feedback effect incorporated with the responsivity of the incident IR can be described. In addition, since the model is based on physics, the model parameters also have their own physical meaning. This analytical model can easily be utilized to describe the temperature and resistance change caused by the applied heat sources and has a unique feature, where it can describe the capability of optical-electro-thermal analysis in the quasi-steady-state, which can hardly be performed with finite element method based thermal analysis tools. The model shows that the temperature of the microbolometer in this study can be increased 7.1% to 18.6% more by the electro-thermal feedback effect.

Acknowledgments

This research was supported by the Academic Research Fund of Hoseo University in 2012 (20120239).

References

1. J. Tissot et al., "High-performance uncooled amorphous silicon video graphics array and extended graphics array infrared focal plane arrays with 17-μm pixel pitch," *Opt. Eng.* **50**(6) 061006 (2011).
2. R. Breiter et al., "Seize, weight, and power reduction of mercury cadmium telluride infrared detection modules," *Opt. Eng.* **50**(6) 061010 (2011).
3. C. Li, C. J. Han, and G. Skidmore, "Overview of DRS uncooled VOx infrared detector development," *Opt. Eng.* **50**(6) 061017 (2011).
4. C. Li, G. Skidmore, and C. Han, "Uncooled VOx Infrared sensor development and application," *Proc. SPIE* **8012**, 80121N (2011).
5. L. Becker, "Influence of IR sensor technology on the military and civil defense," *Proc. SPIE* **6127**, 61270S (2006).
6. A. Fraenkel et al., "Advanced features of SCD's uncooled detectors," *Proc. SPIE* **5957**, 59570N (2005).
7. L. Langof et al., "Advanced multi-function infrared detector with on-chip processing," *Proc. SPIE* **8012**, 80120F (2011).
8. A. Fraenkel et al., "SCD's uncooled detectors and video engines for a wide-range of applications," *Proc. SPIE* **8012**, 801204 (2011).
9. A. Rogalski, "Infrared detectors for the future," *Acta Phys. Pol. A*, **116**(3), 389–406 (2009).
10. D. Murphy et al., "640 × 512 17 μm microbolometer FPA and sensor development," *Proc. SPIE* **6542**, 65421Z (2007).
11. S. H. Black et al., "Uncooled detector development at Raytheon," *Proc. SPIE* **8012**, 80121A (2011).
12. P. Ericsson et al., "Towards 17 μm pitch heterogeneously integrated Si/Ge quantum well bolometer FPAs," *Proc. SPIE* **8012**, 801212 (2011).
13. W. Parrish and J. Woolaway, "Improvements in uncooled systems using bias equalization," *Proc. SPIE* **3698**, 748–755 (1999).
14. E. L. Dereniak and G. D. Boreman, *Infrared Detectors and Systems*, pp. 395–438, Wiley, New York (1996).
15. F. Niklaus et al., "Uncooled infrared bolometer arrays operating in a low to medium vacuum atmosphere: performance model and trade-offs," *Proc. SPIE* **6542**, 65421M (2007).
16. M. Tepegoz, F. Civitchi, and T. Akin, "An optimum reference detector design for uncooled microbolometer FPAs," *Proc. SPIE* **6940**, 694028 (2008).
17. A. Oguz, M. Tepegoz, and T. Akin, "A bias heating cancellation method for resistive uncooled microbolometer detectors," *Proc. SPIE* **7298**, 7298G (2009).
18. S. M. Park and S. Han, "Electro-thermal feedback effects on the signal in a pulse voltage biased μ-bolometer focal plane array," *Trans. KIEE.* **61**(12), 1886–1891 (2012).
19. C. H. Hwang et al., "Readout integrated circuit for microbolometer with an analog non-uniformity correction," *Proc. SPIE* **5987**, 59870P (2005).
20. A. S. Sedra and K. C. Smith, *Microelectronic Circuits*, 3rd ed., pp. 570–645, Saunders College Publishing, Philadelphia (1991).
21. D. Jakonis, C. Svensson, and C. Jansson, "Readout architectures for uncooled IR detector arrays," *Sens. Actuators* **84**(3), 220–229 (2000).

Seung-man Park received his BS (1984) and MS (1986) in physics from Hanyang University, and his PhD (1997) in electrical engineering from the Korea Advanced Institute of Science and Technology (KAIST). He was with the Agency for Defense Development (1987 to 2008), where he led several projects on infrared (IR) detector development. Since 2008, he has been with Hoseo University as a professor. His research interests are IR detector technologies and related systems. He is a member of several professional societies including SPIE.

Seungoh Han received his BS, MS, and PhD in electrical engineering from Korea University in 1996, 1998, and 2006, respectively. Since 2007, he has been with Hoseo University as a professor. His research interests are NEMS/MEMS, smart sensors, and multiphysics modeling.

Hee Chul Lee received his BS (1978) in electronic engineering from the Seoul National University, Korea, and his MS (1986) and PhD (1989) from the Tokyo Institute of Technology, Japan, respectively. Since 1989, he has been with the Department of Electrical Engineering and Computer Science at KAIST and he was the president of the National Nano-Fab Center (NNFC). His research fields include infrared detectors, readout circuits and polymer memories. He is a program committee member of SPIE and has served as a director of many conferences.